A kinematic real-time PPP approach with estimating signal in space range errors

Article *in* Advances in Space Research · June 2024

DOI: 10.1016/j.asr.2024.06.007

Quanrun Cheng
Shanghai Astronomical Observation

Yize Zhang
Chinese Academy of Sciences

Junping Chen
Chinese Academy of Sciences

ARTICLE IN PRESS

Available online at www.sciencedirect.com

ScienceDirect

Advances in Space Research xxx (xxxx) xxx

ADVANCES IN SPACE RESEARCH (a COSPAR publication)

www.elsevier.com/locate/asr

A kinematic real-time PPP approach with estimating signal in space range errors

Quanrun Cheng[a,b], Yize Zhang[a,*], Junping Chen[a,c], Heng Wang[a,d], Bin Wu[e]

[a] Shanghai Astronomical Observatory, Chinese Academy of Sciences, Shanghai 200030, China
[b] School of Astronomy and Space Science, University of Chinese Academy of Sciences, Beijing 100049, China
[c] Shanghai Key Laboratory of Space Navigation and Positioning Techniques, Shanghai 200030, China
[d] Shenyang Aerospace University, Shenyang 110136, China
[e] Shanghai Dahua Surveying & Mapping Technology Co., LTD, Shanghai 201208, China

Received 10 January 2024; received in revised form 27 May 2024; accepted 3 June 2024

Abstract

Since 2013, the International GNSS Service (IGS) real-time service (RTS) has been providing precise orbit and clock corrections for ten years, which enables real-time positioning at the decimeter level. High precision positioning relies heavily on accurate orbit and clock. However, constrained by the relatively short observation duration, the accuracy of real-time products are often worse than the final products. Previous studies indicate that compensating for errors in orbit and clock can improve positioning accuracy. Based on this theory, we proposed an improved positioning model, which incorporates the signal-in-space range error (SISRE) into the ionosphere-free combination observation equation and treats it as a parameter in the Kalman filter. Through the analysis of SISRE, we find that the time-varying characteristic of the parameter follows a random walk assumption. To find the optimal parameter settings of the SISRE parameters, a two-dimensional sensitivity analysis is employed, and a set of recommended values are provided. In the simulated kinematic positioning experiments, the proposed method achieves positioning accuracies of 17.3 cm, 19.6 cm, and 18.0 cm for GPS, BDS-3, and Galileo, respectively, representing a 10–20 % improvement over traditional methods. In real-time PPP experiment, the accuracy reaches 21.7 cm, indicating a 12.9 % improvement compared to traditional methods.

Keywords: Real-time PPP; Signal in space error; Kalman filter; Process noise

1. Introduction

Precise Point Positioning (PPP) is one of the most widely-used approaches for high-precision positioning with the development of global navigation satellite systems (GNSS) (Zumberge et al., 1997). In order to satisfy the needs for real-time data processing and application, the IGS Real-Time Work Group (RTWG) was established in 2001, and started the Real-Time Service (RTS) which has officially operated since 2013 (Chen et al., 2013; Elsobeiey and Al-Harbi, 2016). The RTS provides access to precise orbit and clock corrections products in addition to GNSS data via Radio Technical Commission for Maritime Services (RTCM) and Networked Transport of RTCM via Internet Protocol (NTRIP) (Li et al., 2022). The PPP approach relies heavily on the availability of the high-precision satellite orbit and clock. Errors in orbit and clock

* Corresponding author.
E-mail addresses: chengquanrun@shao.ac.cn (Q. Cheng), zhyize@shao.ac.cn (Y. Zhang), junping@shao.ac.cn (J. Chen), wh18841121030@163.com (H. Wang), wj12832@Sohu.com (B. Wu).

https://doi.org/10.1016/j.asr.2024.06.007

Please cite this article as: Q. Cheng, Y. Zhang, J. Chen et al., A kinematic real-time PPP approach with estimating signal in space range errors, Advances in Space Research, https://doi.org/10.1016/j.asr.2024.06.007

corrections directly impact positioning accuracy. If the errors in orbit and clock can be partially or completely compensated, it would lead to an improvement in positioning accuracy.

In order to compensate for the combined effects of the aforementioned orbit and clock corrections, researchers have already undertaken substantial work. Montenbruck and Ramos-Bosch (2008) proposed an additional parameter to simulate the combined effects of orbit and clock errors, finding this approach effective in orbit determination of earth orbiting satellites. Carlin et al. (2021) applied this approach to PPP based on broadcast ephemeris, demonstrating its effectiveness in positioning process. The additional parameter, which called signal-in-space range error (SISRE) parameter, is estimated along with coordinate parameters, wet part of the tropospheric delay, and ambiguities. The variability of SISRE parameter is described in a random walk model. This method can significantly enhance positioning accuracy when using GPS and Galileo broadcast ephemeris data. The key to this approach is to determine the process noise of the new parameter. Appropriate process noise can further improve positioning accuracy.

The broadcast ephemeris typically undergo periodic updates, making the assumption of a random walk less suitable. Chen et al., (2022a) proposed a method to reset the variance of the SISRE when ephemeris is switch between two IODEs, which partly compensates the accuracy degradation caused by discontinuities, and this method has shown promising results, particularly for BDS-3. Similarly, Xu et al. (2023) applied a method to precise orbit and clock products based on B2b corrections and achieved an improvement of approximately 25 % in kinematic mode. Tang et al. (2023) proposed the application of estimating SISRE in precise point positioning based on predicted ephemeris. They adaptively adjusted the weighting strategy, resulting in accuracy improvements ranging from 15 % to 60 %.

Therefore, estimating SISRE parameter is proved to be effective in compensating ephemeris errors. However, the impact of estimating SISRE on real-time precise positioning remains unclear. With the development of applications such as autonomous driving, the demand for real-time high-precision positioning has become increasingly pronounced. Therefore, investigating the effectiveness of SISRE estimation methods for real-time precise positioning holds practical value. Moreover, given the already high accuracy of real-time precise ephemeris, the effectiveness of SISRE estimation is likely to be inconspicuous or potentially deteriorating to positioning accuracy if the initial values and process noise of SISRE parameters are not accurately configured. In this paper, we conduct further experiments and analysis to address the issues.

First, we provide a detailed introduction to the positioning method. Subsequently, we perform a brief analysis of the real-time orbit and clock accuracy from various analysis centers, which is crucial guidance for the settings of SISRE parameters in Kalman Filter. Then, we conduct simulated kinematic experiments using IGS station observations, and a set of real kinematic data is used for validation as well.

2. Methodology

2.1. Real-time orbit and clock recovery

Generally, real-time state space representation (SSR) corrections can be expressed by the following equation (Yu et al., 2023; Xu et al., 2023)

$$\mathrm{SSR}(t_0, IOD) = (\delta r, \delta a, \delta c, \delta\dot{r}, \delta\dot{a}, \delta\dot{c}, A_0, A_1, A_2) \tag{1}$$

where t_0 is the reference time. IOD is the issue of data ephemeris (IODE). $(\delta r, \delta a, \delta c)$ are the orbit corrections in radial, along-track, cross-track components, respectively. $(\delta\dot{r}, \delta\dot{a}, \delta\dot{c})$ are the velocity of orbit corrections in three components, respectively. (A_0, A_1, A_2) are the polynomial coefficients of clock corrections. Complete orbit correction vector δorb is computed as:

$$\delta orb = \begin{bmatrix} e_{\text{radial}} \\ e_{\text{along}} \\ e_{\text{cross}} \end{bmatrix} \times \begin{bmatrix} \delta r \\ \delta a \\ \delta c \end{bmatrix} + \begin{bmatrix} e_{\text{radial}} \\ e_{\text{along}} \\ e_{\text{cross}} \end{bmatrix} \times \begin{bmatrix} \delta\dot{r} \\ \delta\dot{a} \\ \delta\dot{c} \end{bmatrix} \times (t - t_0)$$
$$\begin{bmatrix} e_{\text{radial}} \\ e_{\text{along}} \\ e_{\text{cross}} \end{bmatrix} = \begin{bmatrix} \frac{\dot{r}}{|\dot{r}|} \times \frac{r\times\dot{r}}{|r\times\dot{r}|} \\ \frac{\dot{r}}{|\dot{r}|} \\ \frac{r\times\dot{r}}{|r\times\dot{r}|} \end{bmatrix} \tag{2}$$

where r,$\dot{r}$ are the satellite positions and velocity vector at epoch t calculated by broadcast ephemeris, respectively. $(e_{\text{radial}}, e_{\text{along}}, e_{\text{cross}})$ are the unit vectors in radial, along-track, and cross-track components, respectively. Finally, the corrected satellite position can be expressed as:

$$X = X_{brdc} + \delta orb \tag{3}$$

Similarly, the satellite clock is corrected as follows:

$$\begin{cases} \delta clk = A_0 + A_1(t - t_0) + A_2(t - t_0)^2 \\ Clk = Clk_{brdc} + \frac{\delta clk}{c} \end{cases} \tag{4}$$

where δclk denotes the correction of the satellite clock; Clk is the precise satellite clock used for precise point positioning; Clk_{brdc} is the satellite clock at epoch t_0 calculated by broadcast ephemeris; and c is the speed of light in meter per second in the vacuum.

2.2. Improved real-time PPP positioning approach

The observation equations for pseudorange and carrier-phase measurements in PPP are based on utilizing precise correction data or models to eliminate unknown terms in the measurement equations. The dual-frequency ionosphere-free combination observations are as follows (Kouba et al., 2017; Chen et al., 2022b)

$$p = \rho + \xi + c(\mathrm{d}t_r - \mathrm{d}t^s) + (T + \mathrm{d}T) + e \quad (5)$$

$$\varphi = \rho + \xi + c(\mathrm{d}t_r - \mathrm{d}t^s) + (T + \mathrm{d}T) + \lambda(A + \omega) + \epsilon \quad (6)$$

where p and φ are the ionosphere-free combination of pseudorange and carrier-phase measurements, ρ is the geometrical range between the satellite's and the receiver's antenna reference points, ξ is the correction of phase center offset for transmitting and receiving antennas, c is the speed of light, $\mathrm{d}t_r$ and $\mathrm{d}t^s$ are the receiver and satellite clock offsets, T is the modeled tropospheric delay, $\mathrm{d}T$ is an additional, estimated tropospheric delay correction, λ is the wavelength of the ionosphere-free combination, A is the float-valued ionosphere-free combination of carrier phase ambiguities, ω is the carrier-phase wind-up, and where e and ϵ are the combined noise and multipath errors for pseudorange and carrier-phase. The user position coordinates x_r , y_r and z_r are included in the geometric range

$$\rho = \sqrt{(x^s - x_r)^2 + (y^s - y_r)^2 + (z^s - z_r)^2} \quad (7)$$

where x^s, y^s and z^s are the coordinates of the satellite.

The observations are processed in a Kalman-filter, which estimates the position, receiver clock offset, and ambiguities $A_0 \ldots A_n$ for n tracked satellites as part of the filter's state vector

$$\underline{x} = [x_r \quad y_r \quad z_r \quad \mathrm{d}t_r \quad \mathrm{d}T \quad A_0 \ldots A_n] \quad (8)$$

The proposed approach, is to include the projected orbit and clock errors as additional parameter into the pseudorange and carrier-phase observation equations as suggested by Carlin et al. (2021)

$$p = \rho + \xi + c(\mathrm{d}t_r - \mathrm{d}t^s) + (T + \mathrm{d}T) + s + e \quad (9)$$

$$\varphi = \rho + \xi + c(\mathrm{d}t_r - \mathrm{d}t^s) + (T + \mathrm{d}T) + s + \lambda(A + \omega) + \epsilon \quad (10)$$

the filter's state vector now is as:

$$\underline{x} = [x_r \quad y_r \quad z_r \quad \mathrm{d}t_r \quad \mathrm{d}T \quad s_0 \ldots s_n \quad A_0 \ldots A_n] \quad (11)$$

where $s_0 \ldots s_n$ are SISRE values for n tracked satellites, reflecting the combined impact of clock errors and the radial component of orbit errors.

In this research, the process noise of $s_0 \ldots s_n$ is treated as random walk parameters in kalman filter. The formula $q = \sigma_p^2 \cdot \Delta t$ is commonly used as a reference for determining the process noise of a random walk. In this context, the unit of σ_p is 'mm/$\sqrt{}$h' and the unit of Δt is 's'. σ_p describes the time-varying characteristics of the parameters and Δt is the interval of position process.

3. Analysis

3.1. Signal in space range error of real-time products

The errors in the ephemeris is composed of two parts: orbit error and clock error. Correspondingly, the definition of SISRE according to Montenbruck et al. (2018) and Chen et al. (2022) is as follows:

$$SIS = \sqrt{(\alpha \cdot R - c \cdot \tau)^2 + \beta^2 (A^2 + C^2)} \quad (12)$$

where A, C, and R are the along-, cross-track, and radial component of orbit error respectively. τ denotes the error of clock. α and β denote the contribution of orbit error to SIS.

Considering that the ephemeris error has a direction and the contributions to the error of the along- and cross-track component are relatively small, we define the SISRE as the following refer to the definition of Zhang et al. (2020)

$$SIS = \alpha \cdot R - c \cdot \tau \quad (13)$$

now, the SIS transforms from a scalar to a vector. In Eq. (13), α has a value of 0.982, 0.984 and 0.980 for BDS-3 MEO, Galileo and GPS satellites (Montenbruck et al., 2018; Chen et al., 2022c). The SISRE obtained from this method is called 'R-Clk'.

In this study, the SSR corrections provided by Deutsches GeoForschungs Zentrum (GFZ) are employed to transform broadcast ephemeris into real-time precise ephemeris. Using a final products (gbm) as a reference, we conducted an analysis of the variations in real-time precise ephemeris. The interval of the data is at 30 s. Due to the fact of specific system time bias between real-time products and final products, a double-differenced method was applied to mitigate this bias (Yao et al., 2017; Montenbruck et al., 2018; Wu et al., 2020). Fig. 1 illustrates the time series of R-Clk for GPS, BDS-3 MEO and Galileo satellites on December 26, 2022. It is evident that each satellite exhibits discernible systematic biases for all three

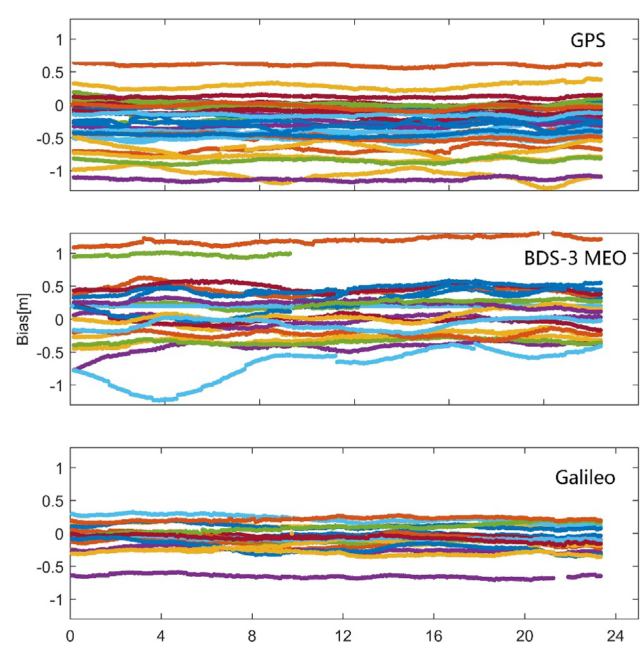

Fig. 1. Time series of R-Clk for GPS, BDS-3 MEO, Galileo on December 25, 2022.

systems. For GPS, these biases typically fall within 1 m, with the majority falling within 0.5 m. In the case of BDS-3, the majority of biases are within 0.5 m, though certain satellites may exhibit biases of up to 1 m. In contrast, Galileo displays notably smaller biases compared to the other two systems, with the majority of satellites exhibiting biases within 0.3 m. The mean RMS biases for R-Clk in the three systems are 0.48 m, 0.39 m, and 0.16 m, respectively. It is evident that these biases exist for each satellite and, except for a few, most of the satellite biases remain near a stable value. The time-invariant portion of the errors caused by these biases will be absorbed by the ambiguities due to their strong correlation, which will not affect the positioning results. However, the time-varying portion will remain in the residuals and impact the positioning results. The new parameters utilized in this paper can estimate this time-varying error as parameters to avoid contaminating the positioning results.

Moreover, it is worth noting that these biases exhibit gradual temporal variations over time. As shown in Fig. 1, the value of R-Clk is not constant but changes over time. By calculating the temporal variation of R-Clk and then determining the probability distribution of this variation, it is expected that this temporal variation should follow a normal distribution. Fig. 2 displays the probability distribution of the first-order difference in R-Clk among different epochs for each system. The interval between epochs is 30 s. The "Limits" mentioned in Fig. 2 are set to $\pm$ 0.5 cm/(30 s). For the GPS and Galileo systems, about 66 % of the results fall within this range. This distribution is essentially equivalent to 1σ (one standard deviation). The situation for BDS-3 differs slightly, with approximately 56 % of variation falling within $\pm$ 0.5 cm/(30 s), which is smaller than that of the other systems. When setting up the parameters, it is recommended to slightly increase the process noise for the SISRE parameter of the BDS-3 satellites. While, the settings for GPS and Galileo should be similar.

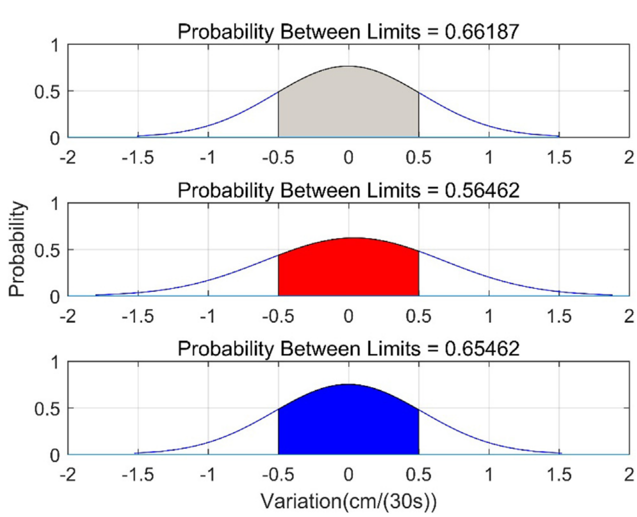

Fig. 2. Distributions of R-Clk Discontinuities from December 25 to 27, 2022: GPS (Top), BDS-3 (Center), Galileo (Bottom). "Probability Between Limits" refers to the probability within 0.5 cm/(30 s).

3.2. Optimal SISRE parameter settings

Appropriate process noise settings of SISRE parameters can impact positioning results, as validated in Carlin et al., 2021. We propose that incorporating the initial standard deviation of SISRE parameters into consideration is more rigorous. Therefore, we utilize a two-dimensional sensitivity analysis to identify the optimal combination of initial values and process noise for SISRE parameters. The premise of this method is that within the search range, there exists an optimal combination that maximizes positioning accuracy.

Fig. 3 illustrates the kinematic positioning accuracy of GPS under different initial values (σ_0) and process noise (σ_p) settings. The dataset used in this study was sourced from seven stations, uniformly distributed globally, as illustrated in Fig. 4. The data covers a period of seven days, from December 25 to 31, 2022. Without a SISRE estimation, the positioning accuracy for this configuration is approximately 17 cm. It can be observed that if parameter settings fall within a certain range, there is an improvement in the positioning results. When the initial value is set to 4 cm, and the process noise is set to 10 mm/$\sqrt{}$h, the positioning accuracy reaches its optimum, at under 14.6 cm. Using the optimal values or settings nearby leads to a noticeable improvement, but if the parameter settings are close to the edges or beyond the boundaries depicted in Fig. 3, the improvement in positioning is marginal, or it may even deteriorate the results. The aforementioned optimal values can be considered as recommended values for GPS, and similar methods can be applied to derive recommended values for other systems.

3.3. Accuracy evaluation of real-time products

Considering the continuous improvement of the GNSS network, IGS started "Multi GNSS Experiment" (MGEX) to integrate tracking and analysis of all satellites navigation systems into IGS activities. Currently, IGS has incorporated a multitude of analysis centers. The real-time SSR corrections from six analysis centers were used for simulated kinematic PPP validation. The satellite systems supported by the analysis centers (ACs), the update intervals for orbit and clock corrections and full name are shown in Table 1. All selected analysis centers support the SSR corrections for GPS. While, CAS, CNE, WHU and SHA provide SSR for BDS-3, and BKG, CAS, CNE and WHU provide SSR for Galileo. All analysis centers, except for BKG, update their orbit and clock corrections at 5 s intervals. The update interval of the analysis center affects the accuracy of the products, but this influence is typically not significant.

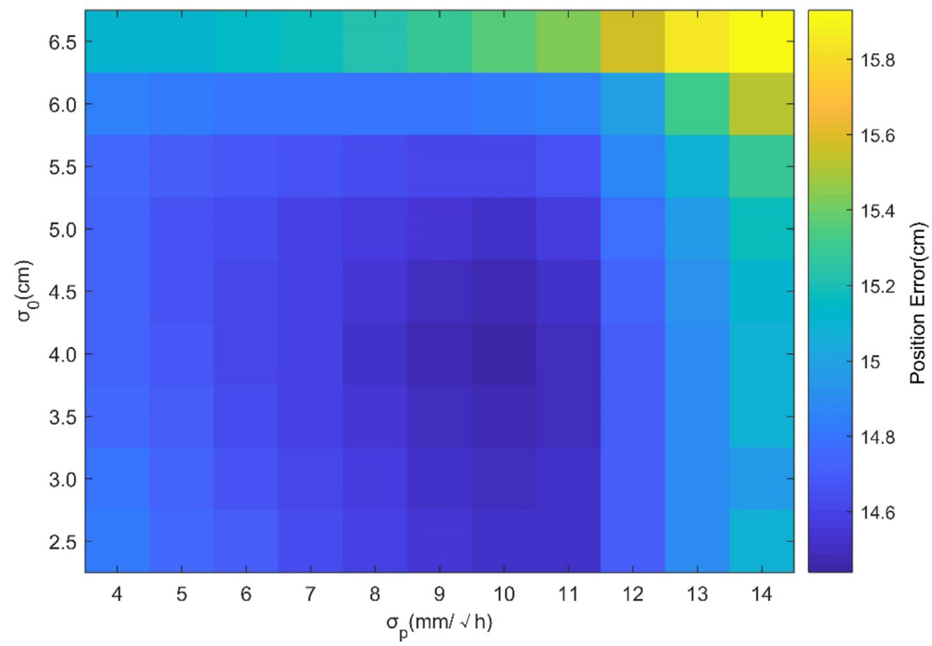

Fig. 3. Heat map of positioning accuracy under different initial values (σ_0) and process noise (σ_P).

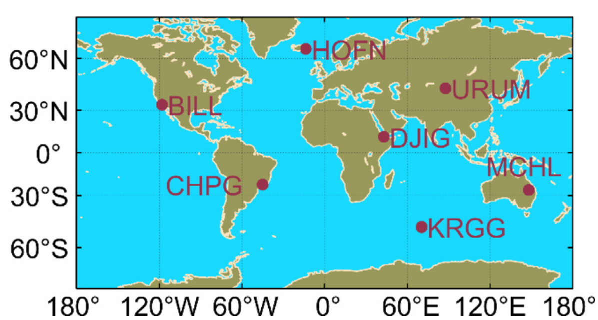

Fig. 4. Site distribution of IGS stations used for PPP validation.

Even if the products provided by the analysis center have high accuracy, there are still subtle differences that need to be considered in the determination of parameter settings. To analyse the differences, we evaluated the accuracy of real-time orbit and clock corrections from several analysis centers, using GFZ's final products as the reference, using data from DOY 330 to 360, 2021. Table 2 displays the SISRE of products from various ACs. The SISRE of BKG, CAS, and SHA is above 4 cm. CNE and ESA achieve accuracy above 3 cm, and WHU achieve the highest accuracy at approximately 2 cm. For BDS-3 MEO, SISRE is around 8 cm for all, but WHU still maintains a significant advantage. Similarly, for Galileo, WHU's products remain the best, with SISRE below 4 cm, while other ACs are around 5 cm. Strictly, it is recommended to determine parameter settings for each different AC. However, considering that various ACs shows similar accuracy for a particular satellite system, it is feasible to determine the settings by systems. We provide a set of reference initial standard deviation and process noise for SISRE parameters. The recommended values are shown in Table 3. In practice, appropriate adjustments can be made around the reference values based on the AC being used. The recommended values are shown in Table 3. These values were obtained using the two-dimensional sensitivity analysis method presented in Fig. 3, which is applicable to the dataset we used for testing. In practice, appropriate adjustments can be made around the reference values based on the AC being used.

Table 1
RTCM-SSR mount points Description.

Products	Systems Supported	Update Interval (Orbit/Clock)	Full Name and Country/Region
BKG	G + R + E	60 s/5 s	Bundesamt für Kartographie und Geodäsie, Germany
CAS	G + R + E + C	5 s/5 s	The Institute of Geodesy and Geophysics (IGG) of the Chinese Academy of Sciences, China
CNE	G + R + E + C + J	5 s/5 s	Centre National d'Etudes Spatiales, France
WHU	G + R + E + C	5 s/5 s	Wuhan University, China
ESA	G	5 s/5 s	European Space Agency, International cooperation
SHA	G + R + C	5 s/5 s	Shanghai Astronomical Observation, China

Table 2
SISRE for each system (unit: cm).

Products	SISRE of GPS	SISRE of BDS-3 MEO	SISRE of Galileo
BKG	4.43	/	5.24
CAS	4.48	8.77	4.92
CNE	3.19	8.28	5.20
WHU	2.34	7.36	3.66
ESA	3.24	/	/
SHA	4.27	8.49	/

Table 3
Optimization of initial value and process noise.

System	Initial standard deviation (cm)	Process noise (mm/$\sqrt{}$h)
GPS	4.0	10.0
BDS-3	8.0	15.0
Galileo	4.0	10.0

4. Simulated kinematic experiment

4.1. Data set

In order to validate the proposed method, we conduct simulated kinematic positioning experiments using IGS station data. Seven globally distributed stations are selected with data from December 25 to 31, 2022, as shown in Fig. 4. The simulated kinematic experiments are divided into two groups. One group uses the traditional real-time PPP mode, without the estimating SISRE, which called 'RT_PPP'. The other group employs the improved method proposed in this research, involving the estimation of SISRE parameters, which called 'RT_PPP_new'. The processing strategies are outlined in Table 4.

4.2. Simulated kinematic PPP results and analysis

Fig. 5 illustrates the comparison between the two positioning methods for GPS. In kinematic experiments, positioning accuracy refers to the root mean square (RMS) of positioning errors from the moment of PPP convergence until the end of the positioning period. The condition for convergence is defined as the positioning error decreasing to within 20 cm and remaining within this limit for ten epochs. The precise coordinates provided in the SINEX (Site Network EXtended) weekly solution file offered by the IGS are used as the reference values.

Overall, all stations exhibit higher positioning accuracy with RT_PPP_new mode. Considering all selected ACs and stations, for RT_PPP mode, the precision in the North and East components is 6.6 cm and 8.2 cm, respectively, while the Up component demonstrates poorer accuracy at 17.3 cm. In RT_PPP_new mode, the precision of the three components is improved to 5.8 cm, 7.1 cm, and 13.2 cm, respectively, representing improvements of 12 %, 13 %, and 24 %. The 3D positioning accuracy has improved from 20.3 cm to 16.1 cm, corresponding an improvement of approximately 21 %. The improvement in positioning accuracy is more significant in the Up component, typically reaching 2 to 6 cm. While, the improvement in the East and North components is relatively small. For those stations with initially high precision, such as the KRGG station, the improvement of RT_PPP_new may be not apparent. It may because the accuracy has reached the limit of RT_PPP_new mode, so further improvements are no longer significant. In contrast, for stations with lower precision, such as the URUM station, the improvement of RT_PPP_new may still be significant.

Table 4
Processing strategy.

Items	Description
GNSS observations	Ionospheric-free combination of GNSS carrier phase and pseudorange, 30 s sampling
Frequencies	B1C & B2a for BDS-3 L1 & L2 for GPS E1 & E5a for Galileo
Elevation cut-off angle	10°
Observables weighting	Comprehensive consideration of satellite system, elevation angle (Zhang et al., 2019)
Orbit and clock product	Real-time broadcast ephemeris + SSR corrections
Processing sessions	Daily solutions of 24 h
Relativistic effect	Corrected (Ashby, 2003)
Solid earth tide	Corrected (Petit and Luzum, 2010)
Ocean tide	Corrected (Petit and Luzum, 2010)
Receiver clock offset	Estimated as white noise
Tropospheric dry delay	Saastamoinen model and Vienna mapping function 1 (VMF1) (Saastamoinen, 1972)
Tropospheric wet delay	Estimated as random walk (2 cm/$\sqrt{}$h) with and Vienna mapping function 1 (VMF1) (Saastamoinen, 1972)
Signal in space range error	Estimated as random walk (refer to Table 3) in proposed approach (RT_PPP_new) and ignored in traditional approach (RT_PPP)
Ambiguity	Estimated as a constant for each ambiguity arc

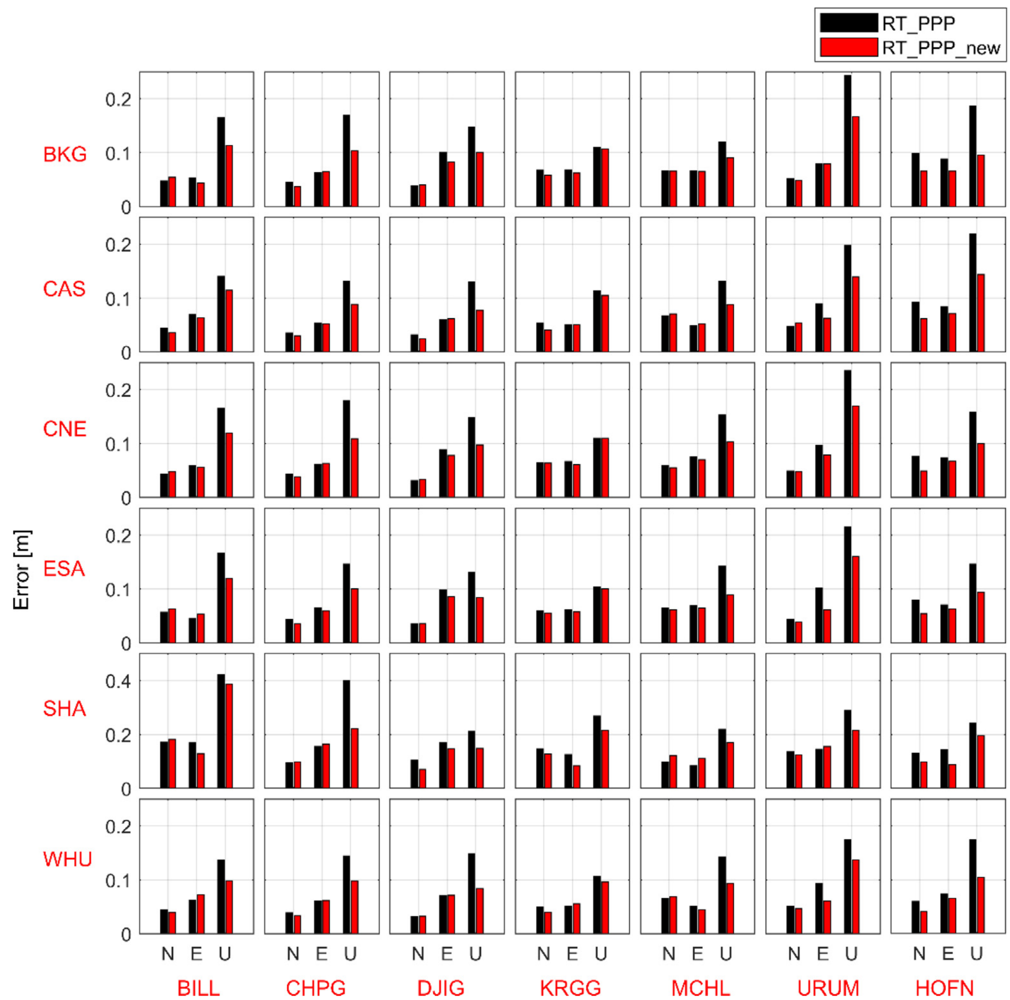

Fig. 5. Positioning accuracy of 6 analysis centers at 7 selected IGS stations for GPS.

Fig. 6 illustrates the precision comparison between the two positioning methods for BDS-3. RT_PPP_new mode still shows better accuracy. For RT_PPP_new, the precision is improved to 10.1 cm, 14.7 cm, and 18.7 cm, respectively, representing improvements of 5 %, 8 %, and 21.8 %. The 3D positioning accuracy has improved from 30.7 cm to 25.8 cm, representing an improvement of approximately 16 %. The 3D accuracy of WHU is 19.6 cm, while CAS and SHA are 28.7 cm and 29.2 cm, respectively. Compared to the other two analysis centers, the results of WHU are better. This aligns with the precision of real-time products.

For Galileo, as shown in Fig. 7. For RT_PPP_new mode, the positioning precision is 6.9 cm, 9.2 cm, and 13.8 cm, respectively, representing improvements of 9 %, 12.4 %, and 17.4 %. The 3D positioning accuracy has improved from 21.1 cm to 18.0 cm, representing an improvement of approximately 14.7 %. Overall, RT_PPP_new mode shows advantages to traditional methods, but when considering stations like BILL or MCHL, precision may be slightly lower than traditional methods when using CAS products, which may cause by the less flexible parameter settings.

Fig. 8 depicts the time series of positioning errors, showing the 24-hour mean positioning error for all ACs and stations utilized by each system. From the figure, it can be observed that the initial positioning accuracy is not influenced by the proposed method. Except for GPS, there is no significant improvement in convergence speed. However, after convergence, the improvements introduced by the proposed method are significant. The positioning error in the RT_PPP_new mode of the three systems is under 0.2 m. This represents a difference from RT_PPP. When RT_PPP mode shows a fluctuation, the influence on RT_PPP_new mode is smaller. This may because the SISRE parameters absorb the influence of outliers such as undetected cycle slips or sudden changes in orbit and clock. Although such errors do not conform to the random walk model, the SISRE parameter still absorbs their influence to some extent.

5. Real-time kinematic experiment

The land vehicle experiment was conducted on Chongming Island in Shanghai, China on October 13, 2023.

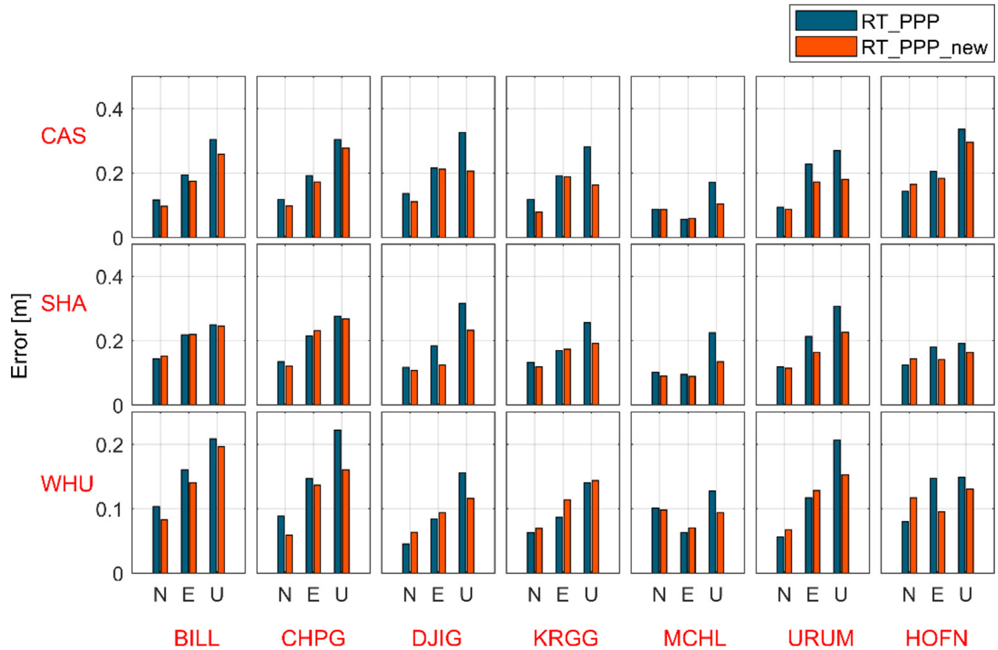

Fig. 6. Positioning accuracy of 3 analysis centers at 7 selected IGS stations for BDS-3.

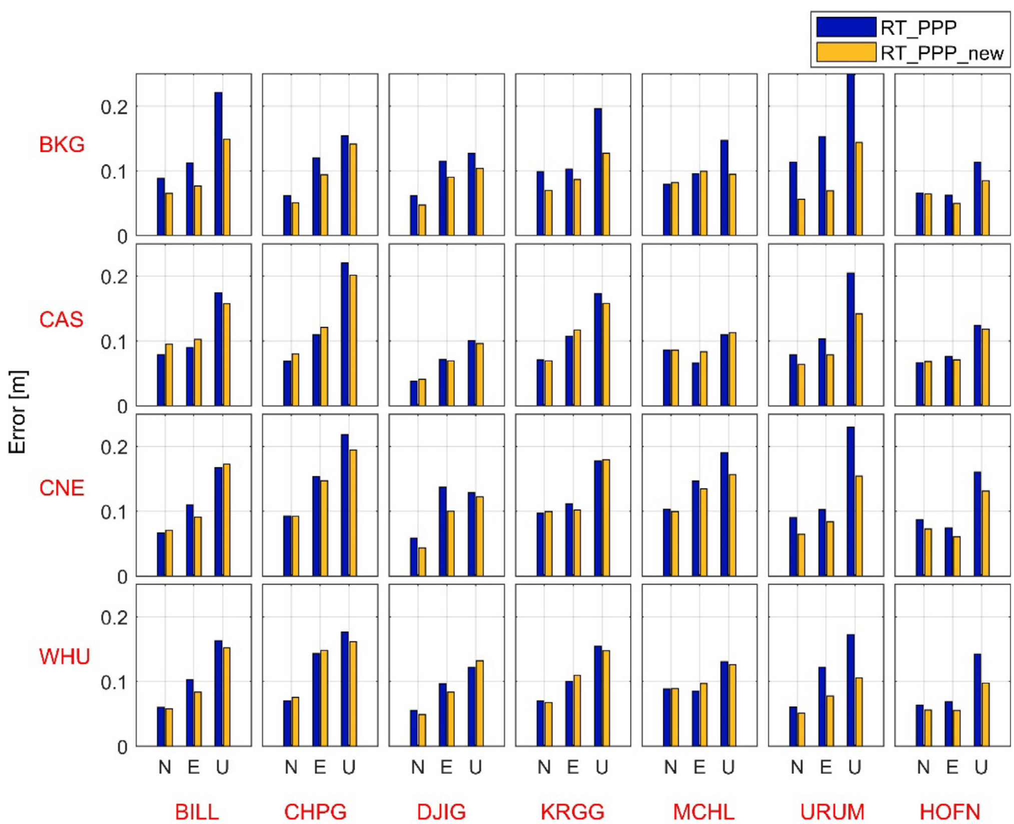

Fig. 7. Positioning accuracy of 4 analysis centers at 7 selected IGS stations for Galileo.

The experiment began and ended at the same location on the western side of the island. The vehicle traveled eastward, following a circular route, and returned to the starting point. Only one lap is designed in the route. The experiment took place from 3:12 PM to 4:32 PM, following China Standard Time (UTC + 8), lasting a total of 1 h and 20 min with an sample interval of 1 s. The test vehicle and trajectory is depicted in Fig. 9. The GNSS receiver at the rover station was the TRIMBLE R750, and the base station employed a CHC N71. Their locations can be seen

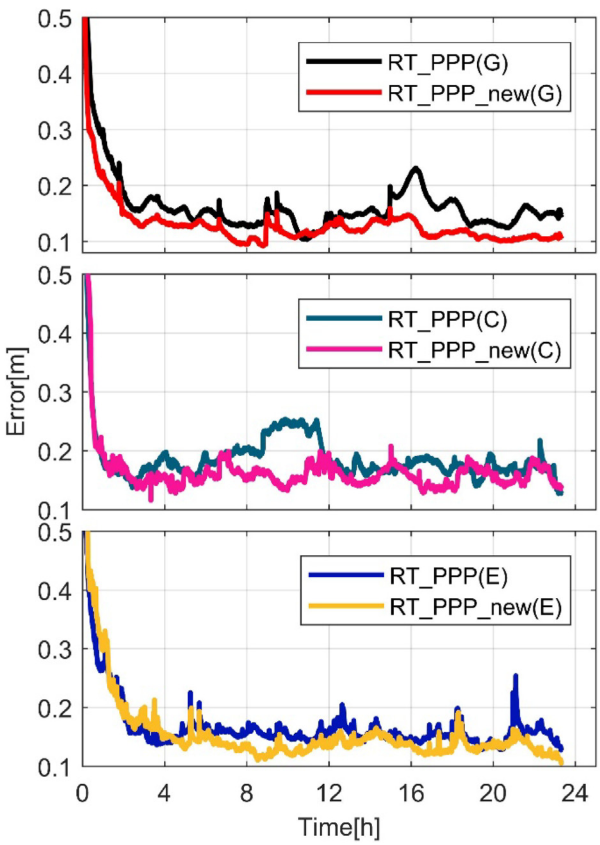

Fig. 8. Position error at different convergence times: Positioning results are a seven-day average of all IGS stations at all analysis centers. The upper, middle, and lower subplots respectively represent GPS, BDS-3, and Galileo.

in the right part of Fig. 9. The positioning results calculated in RTK mode using the Inertial Explorer 8.90 software are taken as the reference. RTK and PPP both utilized dual systems of GPS and BDS-3, with the cutoff elevation angle set to 7°, and the other settings consistent with the simulated kinematic test.

The vehicle started approximately 10 s after the data collection began. Given that the experiment lasted only one hour and twenty minutes, setting the convergence time to one hour could result in the exclusion of most of the useful data. Therefore, we selected 20 min as the convergence time, which allows for the inclusion of the majority of the time period and gives the system sufficient time to converge. According to Fig. 10, there was no significant difference in accuracy between the two methods during the first twenty minutes, so the impact on accuracy statistics is also minimal.

The results of RT_PPP and RT_PPP_new are displayed in Fig. 10, and the number of visible satellites over time during the experiment is displayed in Fig. 11. From the satellite count variation presented in Fig. 11, it is clear that the experimental route on Chongming Island was mostly unobstructed, leading to stable satellite visibility. The number of BDS-3 satellites consistently ranged from 8 to 9, and GPS satellites from 6 to 8, with BDS-3 having an advantage of 2 to 3 satellites over GPS. The total satellite count was around 15, which is sufficient for positioning requirements. Around 15:40, a decrease in satellite count was observed, which corresponded with fluctuations in the accuracy of the positioning error sequence.

With the usage of high-quality receivers and the open environment of Chongming Island, it is reasonable to achieve a high accuracy for RT_PPP mode, with a 3D positioning error of 21.7 cm. RT_PPP_new exhibits superior performance. For the E component, RT_PPP_new has maintained a clear advantage starting from 15:20 through to the end. For the N component, the difference is not as pronounced. The positioning accuracy remains comparable for the initial part, until around 15:45 when RT_PPP_new begins to exhibit a superiority. It can be observed that the errors in the U componant of RT_PPP mode will still exceed 30 cm after convergence, while RT_PPP_new is generally within 20 cm. From a statistical perspective, the positioning errors are 10.4 cm, 8.0 cm, and 13.7 cm for the East, North and Up components for RT_PPP_new mode, showing improvements of 16.1 %, 2.5 %, and 13.8 % compared to the RT_PPP mode.

6. Summary and conclusions

Real-time precise point positioning services are an important application that offers real-time decimeter-level kinematic positioning services to users capable of receiving SSR data streams. Due to limitations in the observation, real-time precise products often exhibit lower accuracy compared to final products. This results in residual

Fig. 9. The left figure shows the test vehicle and its surroundings, and the right figure illustrates the trajectory of the land vehicle-borne experiment.

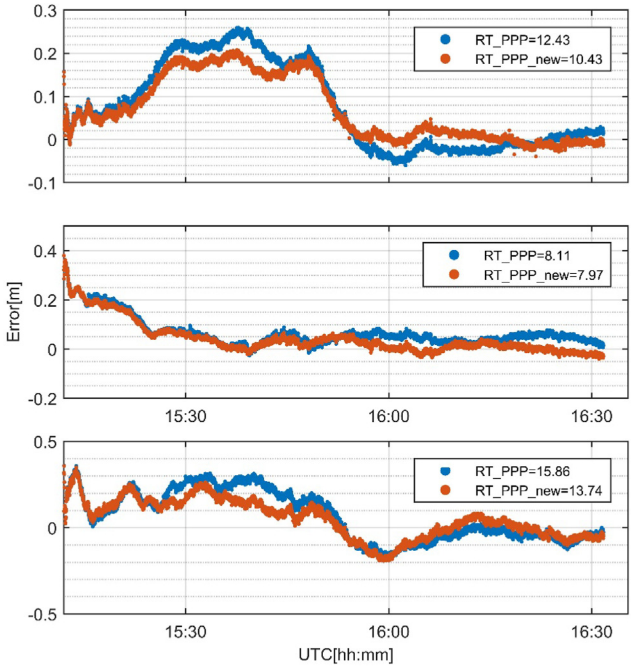

Fig. 10. Positioning error in the land vehicle-borne experiment. The top, middle, and bottom subplots correspond to the East, North, and Up components, respectively.

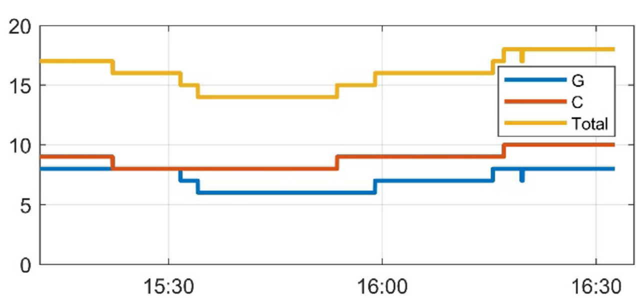

Fig. 11. Variation of the number of visible satellites over time during the vehicle-borne experiment.

decimeter-level errors in orbit and clock offset, which becomes a crucial factor limiting the accuracy of real-time precise point positioning.

In this study, we propose an approach that enhances the traditional ionosphere-free precise point positioning model by considering the biases introduced by orbit and clock errors as parameters. The temporal behavior of the new parameters follows a random walk model. Through sensitivity analysis, we determine the optimal parameter settings for the new SISRE parameters. Real-time precise point positioning experiment based on the proposed method shows an accuracy improvement of over 15 % in simulated kinematic mode. The improvement in the zenith component is particularly pronounced, exceeding 20 %. This conclusion has been validated in the positioning of GPS, BDS-3, and Galileo systems with products from most analysis centers. To validate the practical positioning performance, we conducted experiments to collect real kinematic data on Chongming Island, and the positioning results were similar to those obtained in simulated kinematic mode. The improvements in the East-North-Up components are 16.1 %, 2.5 %, and 13.8 %, respectively.

Considering previous research, the SISRE method has been validated to have good effects in PPP. The method is effective whether using broadcast ephemeris or precise corrections transmitted by B2b. And now, it has been proven to be effective for PPP based on real-time precise ephemerides as well. Additionally, its theoretical model is relatively simple, with minimal computational resource consumption, making it suitable for more widespread applications.

Declaration of competing interest

The authors declare the following financial interests/personal relationships which may be considered as potential competing interests: [The authors declare that there are no conflicts of interest regarding the publication of this paper. This study did not receive any specific grant from funding agencies in the public, commercial, or not-for-profit sectors. There are no financial or personal relationships with other people or organizations that could inappropriately influence (bias) our work.].

Acknowledgements

This research was funded by National Key R&D Program of China (No. 2018YFB0504300); Opening Project of Shanghai Key Laboratory of Space Navigation and Positioning Techniques (No. 202114); National Natural Science Foundation of China, Grant/Award Number: 41904034. Thanks to the GFZ and IGS analysis centers for providing final products and SSR corrections. We also sincerely thank the IGS for the provision of MGEX observations.

References

Ashby, N., 2003. Relativity in the global positioning system. Living Rev. Relativ. 6, 1. https://doi.org/10.12942/lrr-2003-1.

Carlin, L., Hauschild, A., Montenbruck, O., 2021. Precise point positioning with GPS and Galileo broadcast ephemerides. GPS Solut. 25 (2), 77. https://doi.org/10.1007/s10291-021-01111-4.

Chen, J., Li, H., Wu, B., Zhang, Y., Wang, J., Hu, C., 2013. Performance of real-time precise point positioning. Mar. Geod. 36 (1), 98–108. https://doi.org/10.1080/01490419.2012.699503.

Chen, G., Wei, N., Li, M., Zhao, Q., Zhang, J., 2022a. BDS-3 and GPS/Galileo integrated PPP using broadcast ephemerides. GPS Solut. 26 (4), 129. https://doi.org/10.1007/s10291-022-01311-6.

Chen, J., Zhang, Y., Yu, C., et al., 2022b. Models and performance of SBAS and PPP of BDS. Satell. Navig. 3, 4. https://doi.org/10.1186/s43020-022-00065-3.

Chen, J., Wang, J., Yu, C., et al., 2022c. Improving BDS broadcast ephemeris accuracy using ground-satellite-link observations. Satell. Navig. 3, 11. https://doi.org/10.1186/s43020-022-00072-4.

Elsobeiey, M., Al-Harbi, S., 2016. Performance of real-time precise point positioning using IGS real-time service. GPS Solut. 20 (3), 565–571. https://doi.org/10.1007/s10291-015-0467-z.

Kouba, J., Lahaye, F., Tétreault, P., 2017. Precise point positioning. In: Teunissen, P.J.G., Montenbruck, O. (Eds.), Springer Handbook of Global Navigation Satellite Systems, Chap 25. Springer Interna-tional Publishing, Cham, pp. 723–752. https://doi.org/10.1007/978-3-319-42928-1_25.

Li, B., Ge, H., Bu, Y., Zheng, Y., Yuan, L., 2022. Comprehensive assessment of real-time precise products from IGS analysis centers. Satell. Navig. 3, 12. https://doi.org/10.1186/s43020-022-00074-2.

Montenbruck, O., Ramos-Bosch, P., 2008. Precision real-time navigation of LEO satellites using global positioning system measurements. GPS Solut. 12 (3), 187–198. https://doi.org/10.1007/s10291-007-0080-x.

Montenbruck, O., Steigenberger, P., Hauschild, A., 2018. Multi-GNSS signal-in-space range error assessment–Methodology and results. Adv. Space Res. 61 (12), 3020–3038. https://doi.org/10.1016/j.asr.2018.03.041.

Petit, G, Luzum, B, 2010. IERS conventions (2010), IERS technique note 36. Verlag des Bundesamtes für Kartographie und Geodäsie, Frankfurt am Main, Germany.

Saastamoinen, J., 1972. Atmospheric correction for the troposphere and stratosphere in radio ranging satellites. Use Artif. Satell. Geod. 15, 247–251. https://doi.org/10.1029/GM015p0247.

Tang, L., Wang, J., Cui, B., et al., 2023. Multi-GNSS precise point positioning with predicted orbits and clocks. GPS Solut. 27, 162. https://doi.org/10.1007/s10291-023-01499-1.

Wu, W., Guo, F., Zheng, J., 2020. Analysis of Galileo signal-in-space range error and positioning performance during 2015–2018. Satell. Navig. 1, 6. https://doi.org/10.1186/s43020-019-0005-1.

Xu, X., Nie, Z., Wang, Z., et al., 2023. An improved BDS-3 PPP-B2b positioning approach by estimating signal in space range errors. GPS Solut. 27, 110. https://doi.org/10.1007/s10291-023-01455-z.

Yao, Y., He, Y., Yi, W., et al., 2017. Method for evaluating real-time GNSS satellite clock offset products. GPS Solut. 21, 1417–1425. https://doi.org/10.1007/s10291-017-0619-4.

Yu, C., Zhang, Y., Chen, J., Chen, Q., Xu, K., Wang, B., 2023. Performance assessment of multi-GNSS real-time products from various analysis centers. Remote Sens. 15, 140. https://doi.org/10.3390/rs15010140.

Zhang, Y., Kubo, N., Chen, J., Wang, J., Wang, H., 2019. Initial positioning assessment of BDS new satellites and new signals. Remote Sens. 11, 1320. https://doi.org/10.3390/rs11111320.

Zhang, Y., Chen, J., Feng-Yu, C., Ahao, W., Jiexian, W., 2020. Apparent clock and TGD biases between BDS-2 and BDS-3. GPS Solut. 24 (1). https://doi.org/10.1007/s10291-019-0933-0.

Zumberge, J., Heflin, M., Jefferson, D., Watkins, M., Webb, F.H., 1997. Precise point positioning for the efficient and robust analysis of GPS data from large networks. J. Geophys. Res. 102 (B3), 5005–5017. https://doi.org/10.1029/96JB03860.